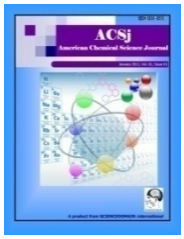

American Chemical Science Journal
4(6): 1014-1031, 2014
ISSN: 2249-0205

SCIENCEDOMAIN *international*
www.sciencedomain.org

Tribological Aspects of Thermally Sprayed Red Mud-Fly Ash and Red Mud-Al Coatings on Mild Steel

Harekrushna Sutar[1*], Subash Chandra Mishra[1], Santosh Kumar Sahoo[1], Himanshu Sekhar Maharana[1] and Ananta Prasad Chakraverty[1]

[1]Department of Metallurgical and Materials Engineering, National Institute of Technology, Rourkela, 769008, Odisha, India.

Authors' contributions

This work was carried out in collaboration between all authors. Author HS designed the study, performed the experiments wrote the protocol and wrote the first draft of the manuscript. Authors HSM and APC managed the analyses of the study. Authors SCM and SKS supervised. All authors read and approved the final manuscript.

Article Information

DOI: 10.9734/ACSj/2014/12691
Editor(s):
(1) Zhi-Cheng TAN, Thermo chemistry Laboratory, Dalian Institute of Chemical Physics, Chinese Academy of Sciences, Dalian, China.
(2) Sang Hak LEE, Professor, Department of Chemistry, Kyungpook National University Daegu, 702-701, KOREA.
Reviewers:
(1) Anonymous, University of Ibadan; Nigeria.
(2) Anonymous, RIEIT, India.
(3) Anonymous, East Point College of Engineering and Technology, India.
Peer review History: http://www.sciencedomain.org/review-history.php?iid=528&id=16&aid=5884

Original Research Article

Received 13th July 2014
Accepted 14th August 2014
Published 25th August 2014

ABSTRACT

The present research work explains the dry sliding wear characteristics of thermally sprayed red mud and its composite coatings. Composite of red mud, fly ash and aluminium are plasma sprayed at 6, 9, 12 and 15 kW operating power levels. The coatings were experimented to study the tribological behaviour like dry sliding wear behaviour, XRD phase transformation, coating thickness, coating morphology, wear

**Corresponding author: Email: h.k.sutar@gmail.com;*

morphology, wear mechanism and co-efficient of friction. 10% Fly ash and 5% aluminium powder were mixed separately by weight with pure red mud and sliding wear test was conducted using pin on disc wear test machine. The test was performed with track diameter of 100 mm and at sliding speed of 100 rpm (0.523 m/s) at a normal load of 20 N. Coating property was discriminated by variation of sliding time length. Operating power was found to be remarkable variable for wear rate, coating thickness, coating morphology and friction coefficient. Significant increase in wear resistance was observed with fly ash and aluminium addition, resulting in an increase in interfacial bond strength and dense film formation.

Keywords: Red mud; fly ash; aluminium; plasma coating; sliding wear behaviour.

ABBREVIATIONS

SEM: Scanning Electron Microscope; FESEM: Filed Emission Scanning Electron Microscope; EDS: Energy Dispersion Spectroscopy; XRD: X-Ray Diffraction; N: Newton; F: Frictional Force in N; μ: Co- efficient of Friction; R: Applied normal load in N; l: Length in mm; Ø: Diameter in mm; ∆m: Mass Loss in mg.

1. INTRODUCTION

In the present scenario coating technologies manifest a promising momentum for emerging materials. Wear resistive coatings claim to be better tribological applications. Surface modification by improving wear resistance is most widely adopted by plasma spraying technique, which could affirm a great versatility and its application to a wide spectrum of materials. Wear resistive coatings can protect against different wear mediums like abrasive, adhesive and corrosive. Some common wear resistive coating materials are nickel, iron, cobalt and molybdenum based alloys, carbides of ceramic and tungsten [1-2]. Investigations pertaining to the erosion wear behaviour of plasma sprayed ceramic coatings by using Taguchi Technique being reported [3]. Evaluation and characterization of plasma sprayed Cu slag-Al composite coatings on metal substrates has been outlined [4].

In retrospection, literatures made available regarding the wear behaviour of WC with 12% Co coatings produced by Air Plasma Spraying method at different standoff distances [5]. Examinations on the basis of the wear behaviour of Mo and Mo+NiCrBSi thermally sprayed coatings being performed for the application as next generation ring face coatings [6]. Almost all plasma sprayed ceramic coatings portrayed favourable tribological performance in linear contact at high temperatures: high anti-wear resistance and easy to be lubricated owing to the oil storage of pores in coatings [7-9]. But needful to say, plasma sprayed ceramic coatings exhibit some failure mechanisms during sliding such as plastic deformation, brittle fracture and polish effects [10], which in turn demands a few additives, which could reduce the friction and wear of plasma sprayed ceramic coatings [11].

Several factors may influence the tribological behaviour of a coated surface ramified as: the geometry of the contact including macro geometry and topography of the surfaces; the material characteristics; basic mechanical properties as well the microstructure and finally the operating parameters controlling the coating deposition [12].

Red mud as an industrial waste material is considered to be the material of choice for coating applications. It is behoving to mention here that, red mud in present decade should be considered as an alternative wealth for replacing some conventional expensive coating materials. Utilization of red mud and its implications made available in literature [13] in great details. Few results on the basis of wear behaviour of red mud were being reported by some researchers. In addition to above, morphology and solid particle erosion wear behaviour of red mud and fly ash composite were being available in literature [14]. Characteristics of plasma sprayed pure red mud coatings were being reported [15]. Red mud as filling material is also found to be the wear enhancing agent for metals [16].

Data pertaining to dry sliding wear behaviour of fly ash and aluminium added red mud composite coatings are not available in literature and needs to be addressed. The present investigation is an attempt to report the wear behaviour of fly ash, aluminium and red mud composite coatings at different operating power subjected to normal laboratory conditions.

2. MATERIALS AND METHODS

2.1 Formulation of Coating Precursor

The coating powder was formulated considering the raw materials as red mud (RM), fly ash (FA) and aluminium (Al). The powder mixture made up of red mud and different percentage of fly ash and aluminium was being prepared separately. In addition, pure red mud powder was also considered as coating material for the sake of comparison analysis. Coating of the various combinations of mixed powders was conducted on one side cross section of the mild steel substrate. Table 1 shows the detail amalgam of the powder composite.

Table 1. Powders used for coating deposition

Sl.no.	Coating material	Mixture composition (by weight %)
1	Red Mud	100
2	Red Mud +Fly Ash	90 + 10
3	Red Mud +Aluminium	95 + 05

The primary raw material as red mud was collected in powder form from National Aluminium Company (NALCO) located at Damonjodi in the state of odisha, India. The as-received powder was sieved to obtain particles in the required size range of 80-100 µm. Raw fly ash was collected from the captive power plant of Rourkela steel plant, India and sieved to maintain the same size range as that of red mud powder. Aluminium powder is procured from Rourkela market and sized to the same size range. Coating powders were extensively prepared by thorough mixing using V shaped blender.

2.2 Development of Substrate

The principal source for substrate preparation is mild steel rod available commercially. The bar was chopped to l = 42 mm and Ø= 15 mm each. The test pieces were grit blasted from one side cross section at a pressure of 4 kg/cm^2 using alumina grits of grit size 80. The dead lock distance in the shot blasting was in-between 120-150 mm. The mean roughness of the cross sections was found to be 5.8 µm. Hereafter the sample pieces are scrubbed in an ultrasonic cleaning unit followed by immediate plasma spraying.

2.3 Plasma Spraying Operation

Plasma spraying was headed up at the Laser and Plasma technology division of Bhabha Atomic Research Centre, Mumbai, India by arrogating conventional atmospheric plasma spraying (APS) set up. The plasma input power was ranged from 6 to 15 kW by steering the gas flow rate, voltage and arc current. The powder feed rate was maintained to be constant at 15gm/min by using a turntable type volumetric powder feeder. Plasma generation demanded the suitability by purging Argon as primary and Nitrogen as secondary gas agent. Spraying was done at an angle of 90º by maintaining the powder feeding as external to the gun. The detailed operating parameters are revealed in Table 2.

Table 2. Operating parameters during coating deposition

Operating parameters	Values
Plasma arc current (Ampere)	200,225,250,300
Arc voltage (Volt)	30,40,48,50
Torch input power (kW)	6,9,12,15
Plasma gas(Argon), (litre/min)	20
Secondary gas (Nitrogen), (litre/min)	2
Career gas(Argon) Flow rate (litre/min)	7
Powder feed rate (gm/min)	15
Torch to base distance (mm)	110
Arc length range (mm)	2,3,6,8,11

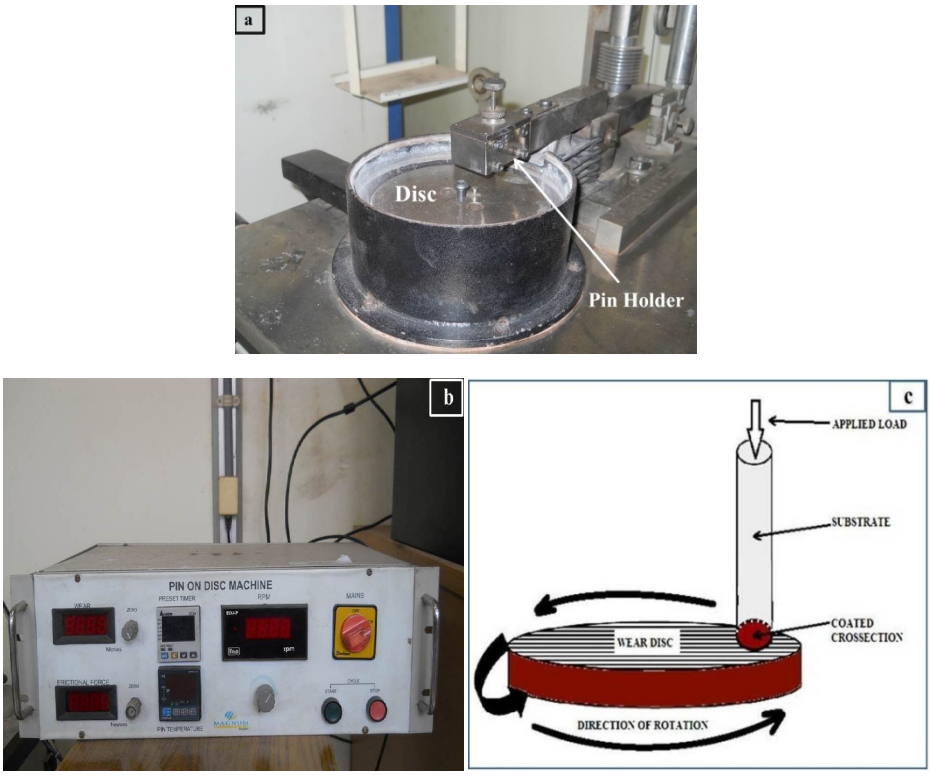

Fig. 1. Comprehensive outline of pin on disc machine

2.4 Pin on Disc Wear Trial

The experiments were conducted using a pin on disc type friction and wear monitor allotted by MAGNUM Engineers, Bangalore, India. The detailed experimental set up is materialized in (Fig. 1a above). The tool possesses a data acquisition system (Fig. 1b above). The concerned machine was used to evaluate the wear behavior of the coatings against hardened ground steel disc (En-32) having hardness of 65 HRC and surface roughness (Ra) 0.5 µm. The gadget is designed so as to study the wear behavior both at lubricated and un-lubricated sliding condition, which occurs between a stationary pin and a rotating disc.

A D.C motor is implicated for rotating the disc with range of speed from 0-250 rpm with wear track diameter 0-150 mm; yielding a sliding speed of 0-15 m/s. Dead weight was applied on the pin by means of pulley and string arrangement. The system has a maximum loading capacity of 400 N. The device is fabricated to keep the pin specimen stationary and perpendicular to disc, while the circular disc spins anti clockwise as shown in (Fig. 1c above).

3. RESULTS AND DISCUSSION

3.1 SEM and EDS Analysis of Precursor and Coatings

A SEM (JEOL; JSM-6480 LV) was epitomized to outline the red mud. The SEM image and EDS analysis of pure red mud powder were manifested in (Fig. 2). The atomic and weight % of elements existent in pure red mud powder is laid in (Table 3). The EDS analysis of red mud revealed the existence of elements like Fe, Al, Si, O and some other minor constituents. The key constituent of red mud was proved to be iron and with its oxides. The EDS analysis of red mud with 10% fly ash coatings prepared at 6 kW of operating power was shown in (Fig. 3). The corresponding elemental analysis was reported in (Table 4), indicating the increase in silica and iron components in the composite coating. The EDS analysis for red mud and 5 % aluminium composite coating made at 6 kW operating power level is shown in (Fig. 4). The elemental analysis analogous to (Fig. 4) was reported in (Table 5), indicating the increase in aluminium content.

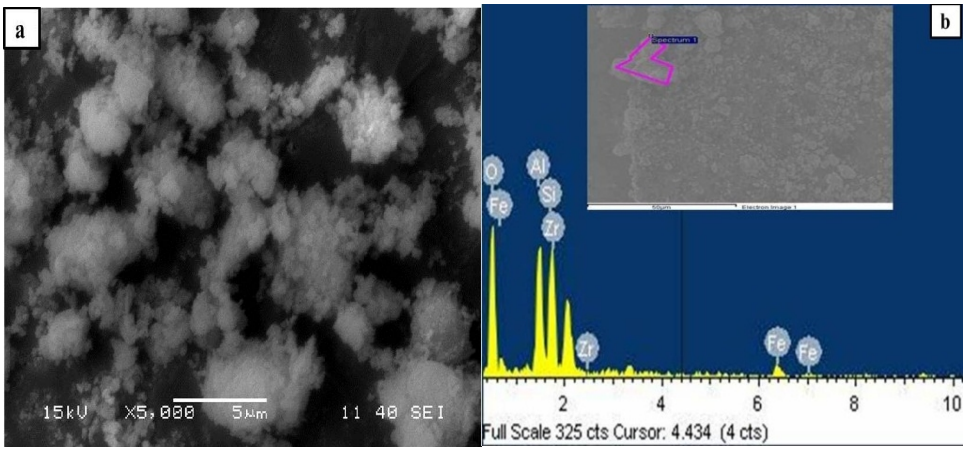

Fig. 2. (a) SEM and (b) EDS analysis of red mud

Table 3. Elemental analysis of red mud

Element	Weight%	Atomic%
C K	24.59	33.29
O K	21.65	24.54
Al K	9.41	4.47
Si K	11.21	7.07
Fe K	33.14	30.62
Totals	100.00	

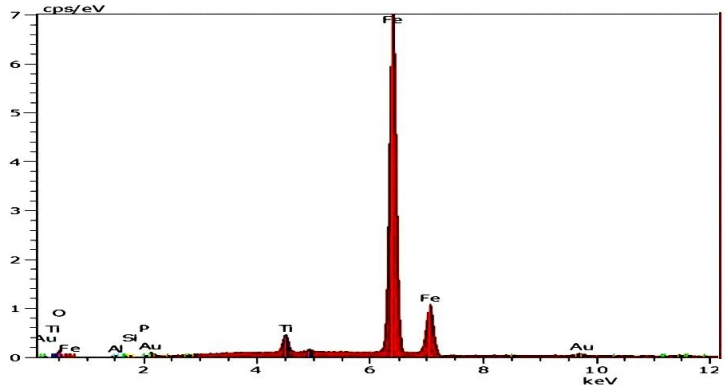

Fig. 3. EDS analysis of RM+10 % FA Composite coating at 6kW

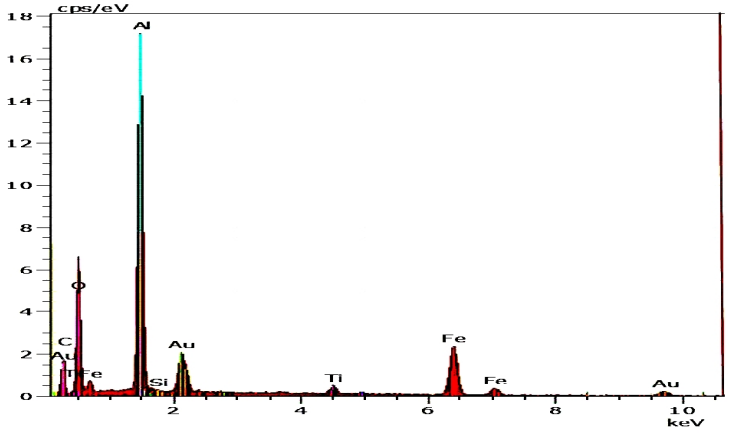

Fig. 4. EDS analysis of RM+ 5 % Al Composite coating at 6 kW

3.2 XRD Analysis of Red Mud and Coatings

To ascertain the phases present and phase changes taken place during plasma spraying, the X-ray diffractograms were captured for red mud powder and its composite coatings using a Philips X-ray diffractometer. The XRD result for red mud powder is shown in (Fig.5).The major phases of red mud powder such as Silicon dioxide (SiO_2), Calcium Alumino ferite ($Ca_2Fe_{1.28}Al_{0.75}O_5$), Hematite ($Fe_2O_3$), Titanium dioxide ($TiO_7$) and Aluminide ($AlFe_3$) were noticed.

Table 4. Elemental analysis of RM+10 % FA Composite coated at 6 kW

Element	Weight %	Atomic %
Fe K	38.13	25.90
O K	21.74	42.61
Ti K	14.02	9.18
Si K	15.10	7.93
Al K	6.59	7.66
Cr K	2.14	1.29
C K	1.99	5.20
Ca K	0.29	0.22
Au K	0.00	0.00
Mg K	0.00	0.00
Totals	100 %	100

Table 5. Elemental analysis of RM+5 % Al Composite coated at 6kW

Element	Weight %	Atomic %
Fe K	39.13	26.89
O K	22.74	41.61
Ti K	9.00	9.18
Si K	14.10	7.93
Al K	11.61	5.46
Cr K	1.14	2.39
C K	1.99	5.20
Ca K	0.29	0.22
Au K	0.00	0.00
Mg K	0.00	0.00
Totals	100 %	100

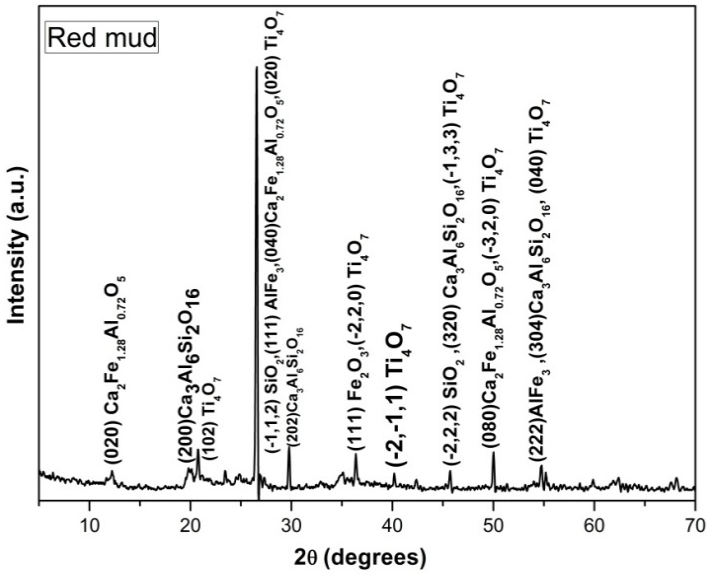

Fig. 5. XRD of Red Mud Powder collected from NALCO

For red mud with 10 % fly ash coatings at 6 and 12 kW operating power level the XRD patterns are shown in (Fig. 6). For 6 kW power level (Fig. 6a) the major phases are silicon aluminium oxides ($Si_{0\cdot9016}Al_{0\cdot0984}O_2$), whereas for 12 kW power level (Fig. 6b) the major phase is changed to pyrophosphate ($NaFeP_2O_7$).

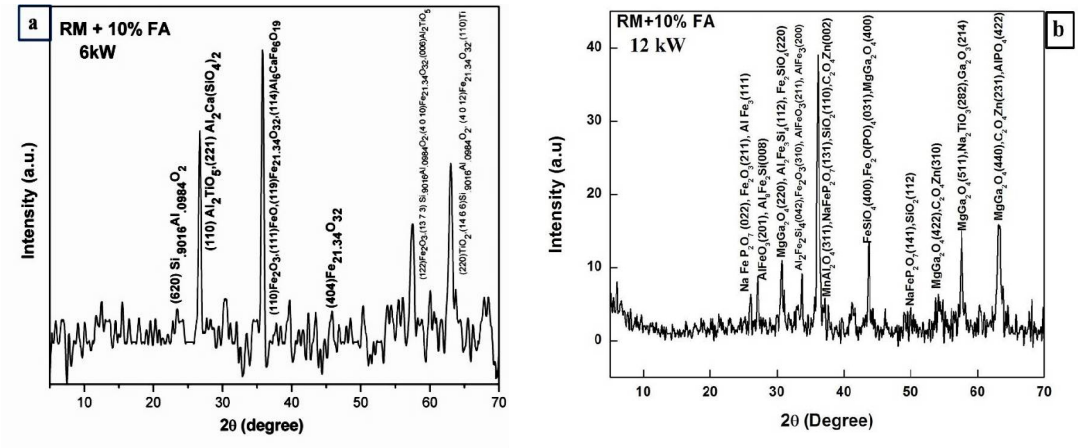

Fig. 6. XRD of RM + 10 % FA Coatings; (a) 6 kW, (b) 12 kW

XRD patterns differentiated for red mud with 5 % aluminium coating is shown in (Fig. 7). At 6 kW operating power level (Fig. 7a) the major phases are silicon dioxide (SiO_2), hematite and aluminium are observed, whereas for 9 kW (Fig. 7b) the major phases changed to calcium carbonate ($CaCO_3$), magnesium oxides (MgO) and manganese oxides (MnO_2). Again for 12 kW power level (Fig. 7c) the major phases found are Calcium Carbonate and Hematite. Significant changes in phases are perceived for 15 kW operating power level. Most of the elements have formed oxides like aluminium iron oxides ($AlFeO_3$) and other elemental oxides as perceptible in (Fig. 7d).

3.3 Investigation of Coating Morphology

The coating surface morphology depends on inter particle bonding of the sprayed powders and coating surface adherence [17]. In case of red mud and 10 % fly ash composite coating the surface morphology deposited at different operating power level are presented in (Fig. 8) implementing FESEM (Nova Nano SEM-450).For coating made at 6 kW, the morphology (Fig. 8a) shows non uniform distribution of bigger globular particles. Cavitation is observed, which may be originated at the time of solidification of particles. As the power level increases the structural pattern significantly affected. Smaller globular particles and more flattened regions are observed indicating proper melting of the particles during spraying. Cavitation decreases and uniformity is improved. This might be due to the proper particle to particle bonding and improved stacking rate to the substrate, which have been resulted in increased interfacial bond strength and more dense film at boundary.

The coating morphology for red mud with 5 % aluminium is visible in (Fig. 9). In this case the operating power has no significant effect on structural properties. For all operating power level small globular grains are seen and fused together to form a splat area. Very few cavities are seen, might be originated at inter particle boundary regions. Addition of

aluminium to red mud might have helped in joining of molten particles during in flight traverse as aluminium remains in molten state for longer time after leaving plasma jet.

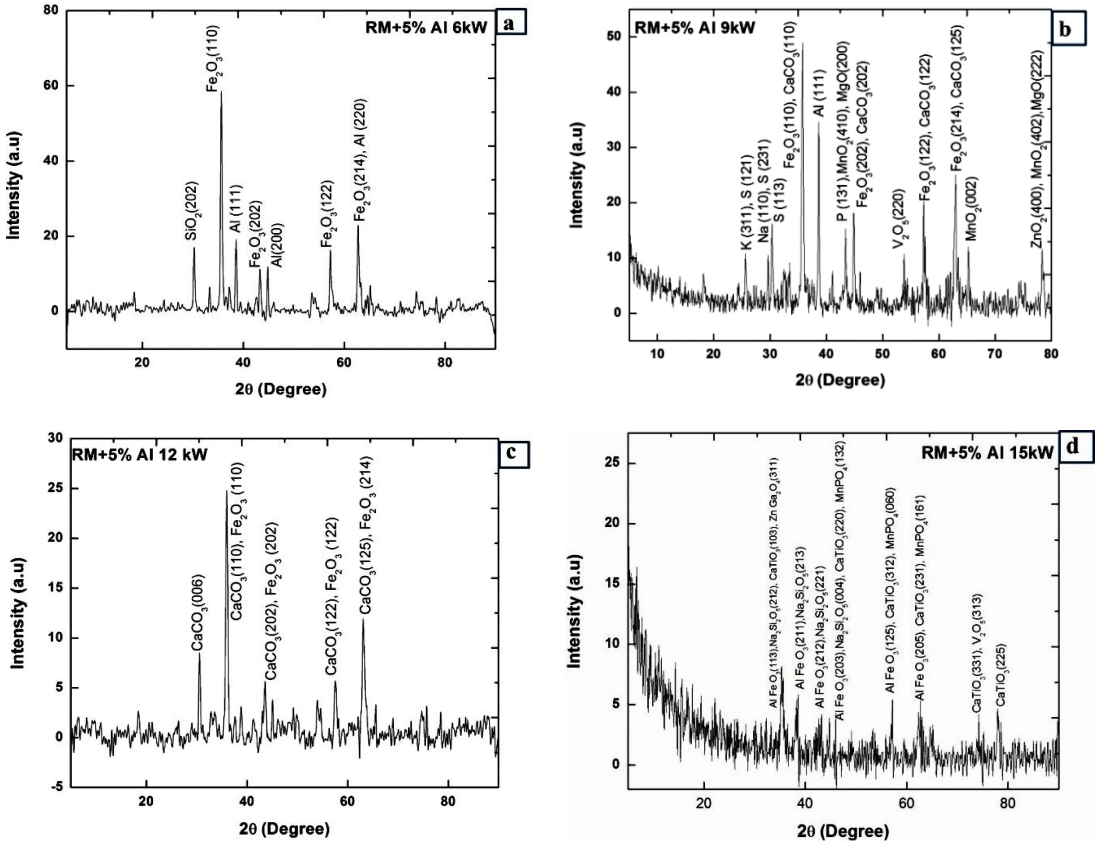

Fig. 7. XRD of Red Mud + 5 % Al; Coatings (a) 6 kW, (b) 9 kW, (c) 12 kW, (d) 15 kW

3.4 Investigation of Coating Thickness

Thickness of Red Mud + 5 % aluminium coatings on mild steel substrate are measured on polished cross-sections of the samples using FESEM. Five readings were taken on each sample and the values are averaged. The mean coating thickness is increased with operating power. The minimum coating thickness is found to be 195 µm for 6 kW operating power. The maximum coating thickness is reported to be 873 µm for 15 kW power. Results are revealed in (Fig. 10). With increase in power level thermal flux increases, this increases the enthalpy of the system. When feed material passes through plasma most of the precursor powder particles get melted and also some disintegrated which flies off. The molten particles which are at much higher temperature when strikes the substrate get splatted and deposition volume increases thereby causing the rise in coating thickness with power. The influence of operating power level on coating thickness is graphically represented in (Fig. 11).

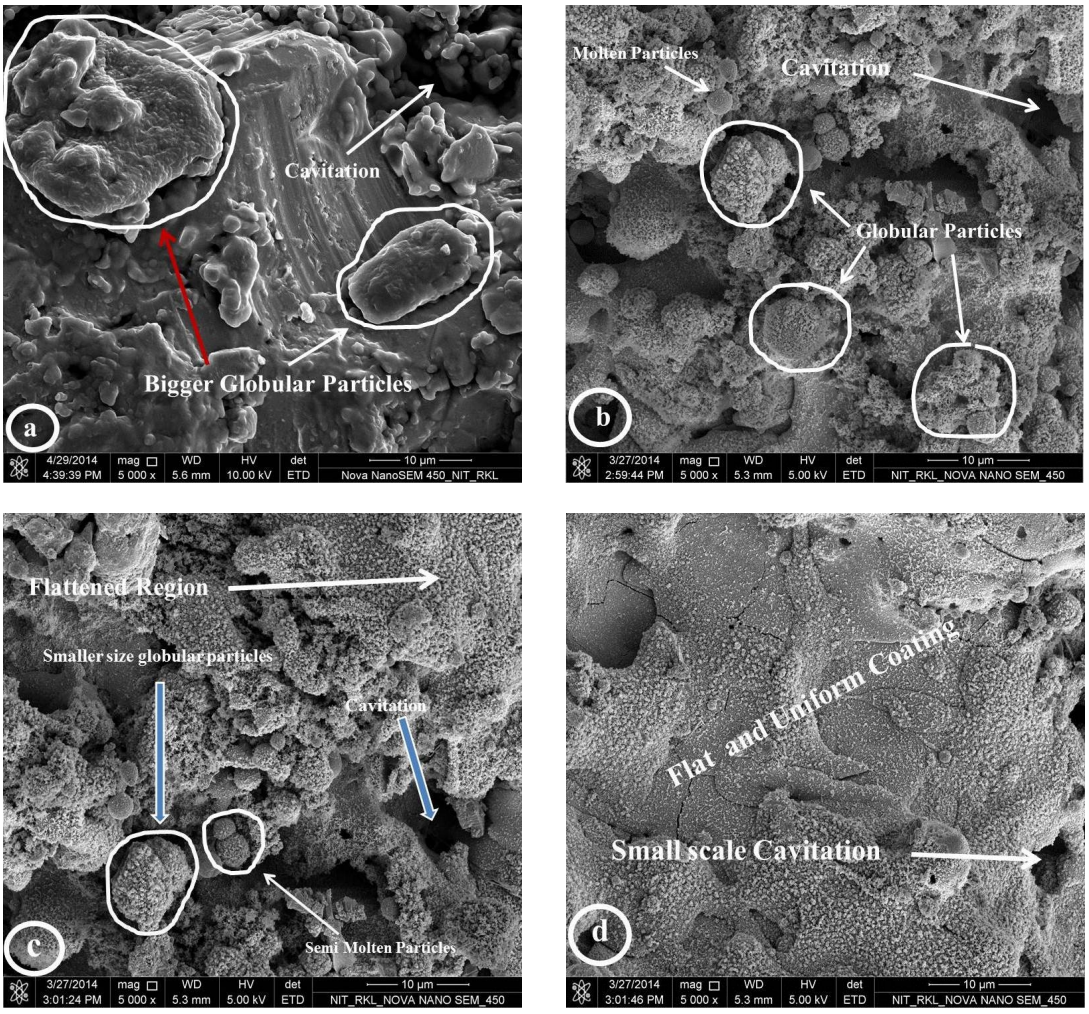

Fig. 8. Coating Morphology for RM + 10 % FA; (a) 6 kW, (b) 9 kW, (c) 12 kW (d) 15 kW

3.5 Diagnosis of Sliding Wear Rate

At incipient, the pin and disc surfaces are polished duly with emery papers for ensuring a smooth contact with coating samples. The wear tests were conducted as per ASTM G-99 standard for different time range under un-lubricated (dry) condition in a normal laboratory condition at ambience temperature and relative humidity. The specimens were weighed before and after each wear test by using electronic weighing machine with accuracy up to second decimal limit (0.001 mg). Specimens were taken care of in particular by cleaning with woolen cloth to avoid entrapment of wear debris and to maintain a distinct wear mechanism. The specimens were cleaned with tetrachloroethylene solution before and after each test. Wear rate was expressed as mass loss (Δm) of the coated specimen after each test. Co-efficient of friction was assessed using the correlation F = µR [18];

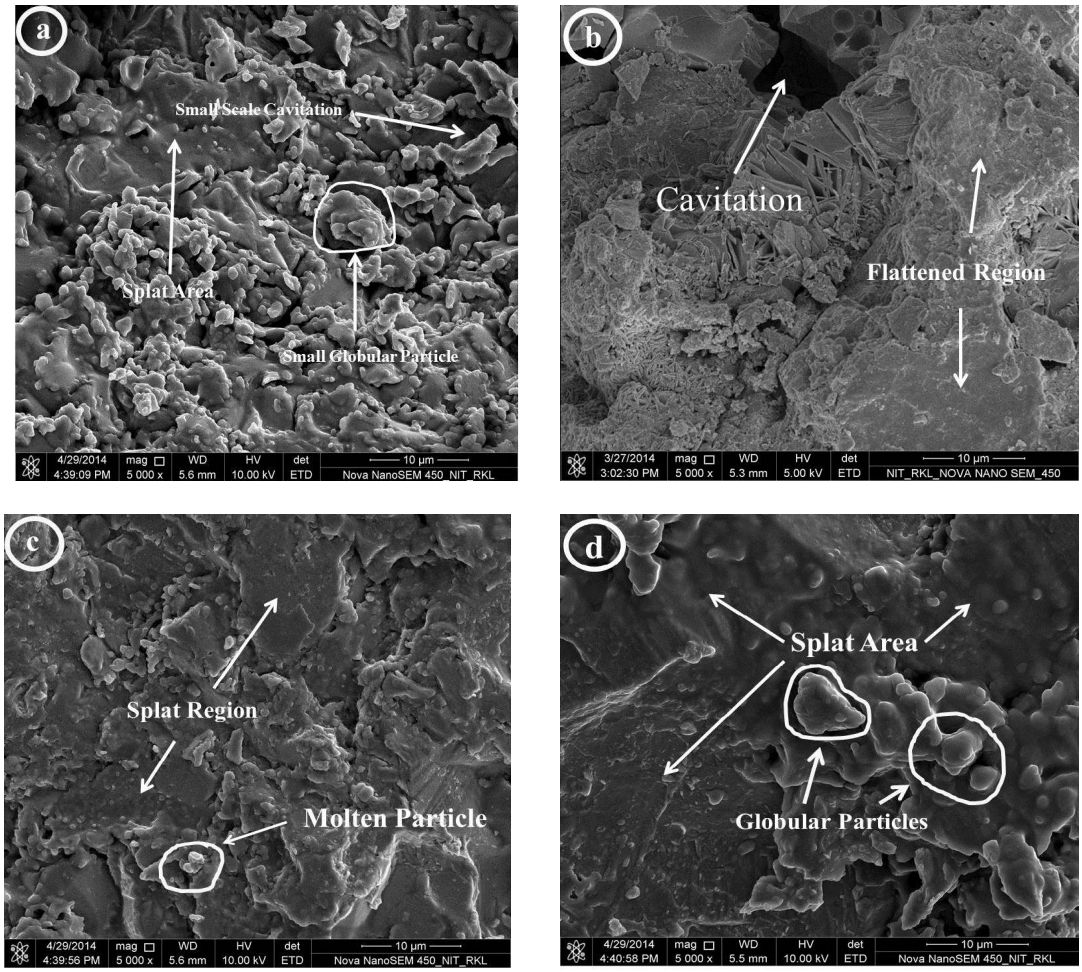

Fig. 9. Coating Morphology for RM + 5 % Al; (a) 6 kW, (b) 9 kW, (c) 12 kW (d) 15 kW

Where F is frictional force in N. R is applied normal load in N. μ is co-efficient of friction. The frictional force (F) was quantified directly from the data acquisition tool in N at each time intervals.

All wear experiments were carried out at a constant normal load of 20 N and a fixed speed of 100 rpm (0.523 m/s).The track diameter was fixed at 100 mm. The total duration of sliding time was retained according to the extent of coating layer occurrence. The minimum and maximum duration of sliding time was 54 and 90 minutes respectively.

The first step of the experiment includes the sliding wear of pure red mud coatings for different operating power level. Mass loss against sliding time is pictured in (Fig. 12). The total duration of sliding time prevails up to 54 minute. At beginning, up to 6 minute a moderate mass loss was observed. Afterwards from 6 to 36 minute a steady mass loss was detected. Then the situation of constant mass loss initiates and titled as break-in phase. The break-in phase continues up to end of the experiment.

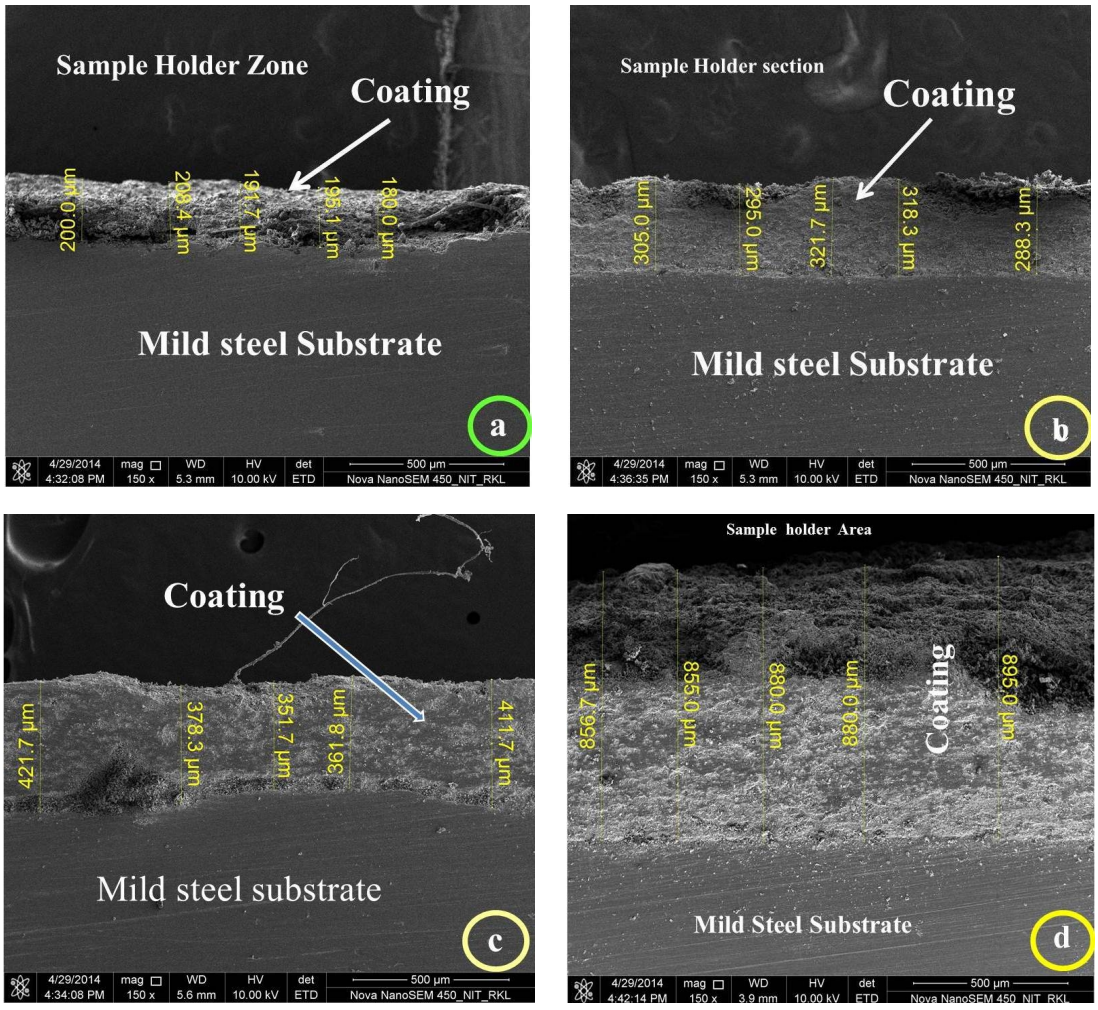

Fig. 10. Snapshot of Coating thickness for RM + 5 % Al (a) 6 kW, (b) 9 kW, (c) 12 kW, (d) 15 kW

It is interesting to notice that the mass loss rate declines with increasing operating power level up to 12 kW. This is the optimum power level in our experiment. For 15 kW power level the mass loss rate lies in between 9 and 12 kW. This is surprising and not obvious, may be due to improper particle to particle bonding and poor stacking to the substrate which in turn lowered the hardness as well as density due to poor interfacial bond strength formation at border line.

(Figs. 13 and 14) represents the mass loss against sliding time for Red Mud + 10 % FA and Red Mud + 5 % Al respectively considering all coating power level. The optimum power level for minimum mass loss lied as the same as earlier for all coating type. The results are differentiated by sliding time length and reaching the break-in phase in behind time. For Red Mud + 10 % FA coating the sliding time prevailed up to 75 minute with break-in phases launched at 54 minute. Whereas for Red Mud + 5 % Al coating the sliding time continued up to 90 minute and break-in phase originated at 66 minute.

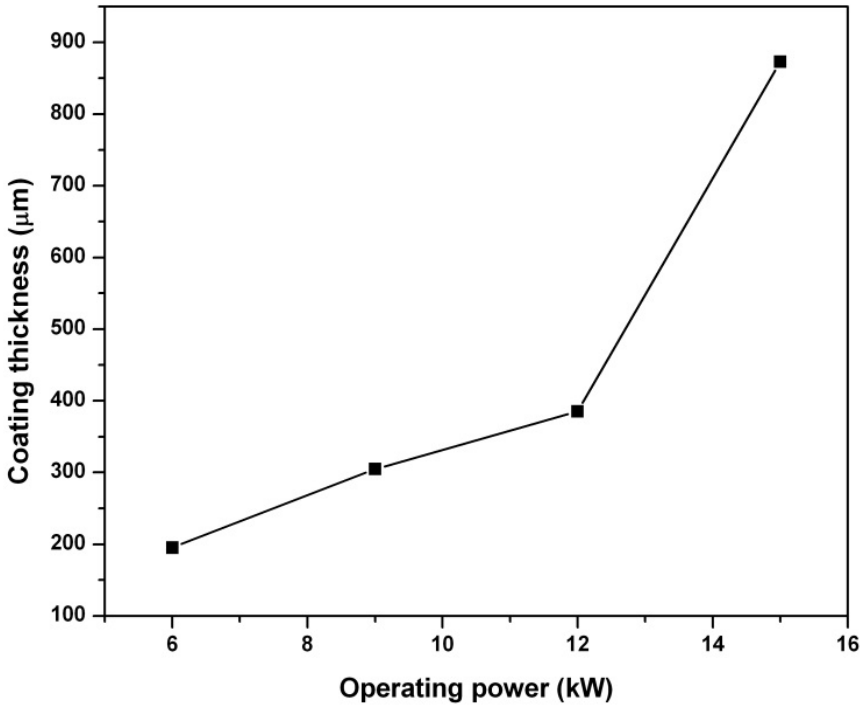

Fig. 11. Graphical presentation of RM+5% Al composite coating thickness with operating power

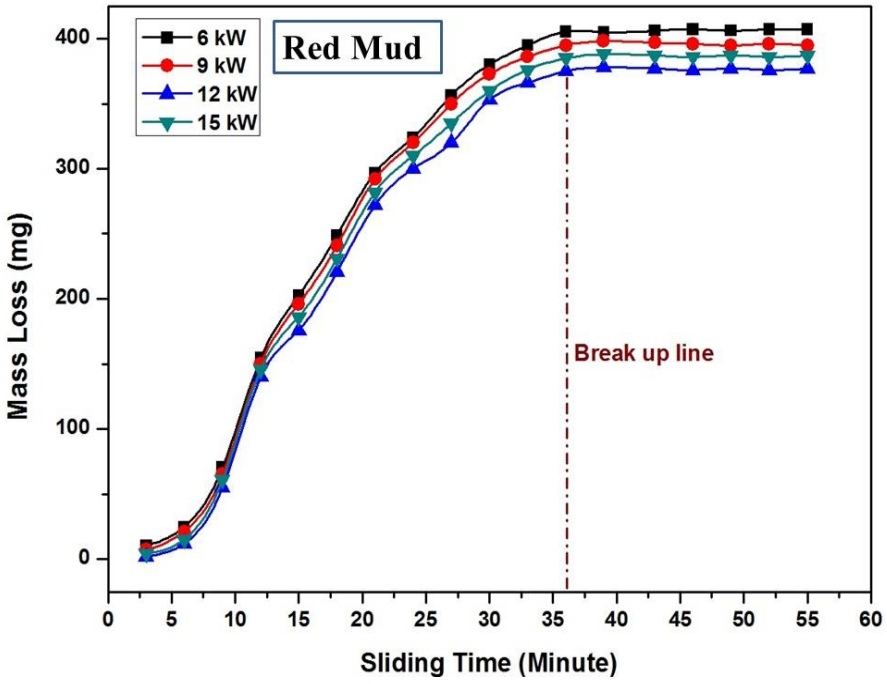

Fig. 12. Mass loss curves for red mud

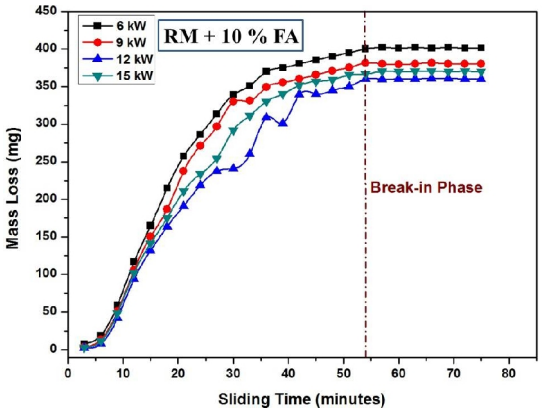

Fig. 13. Wear plot for RM + 10 % FA

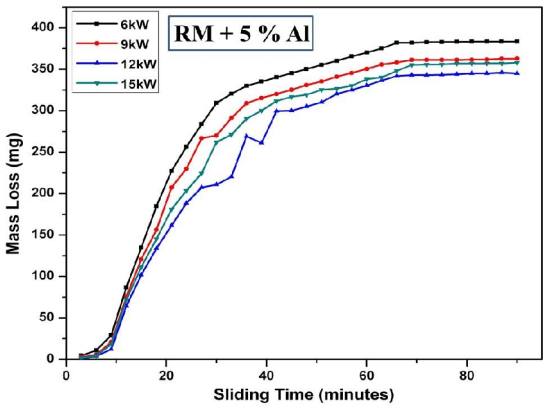

Fig. 14. Wear plot for RM + 5 % Al

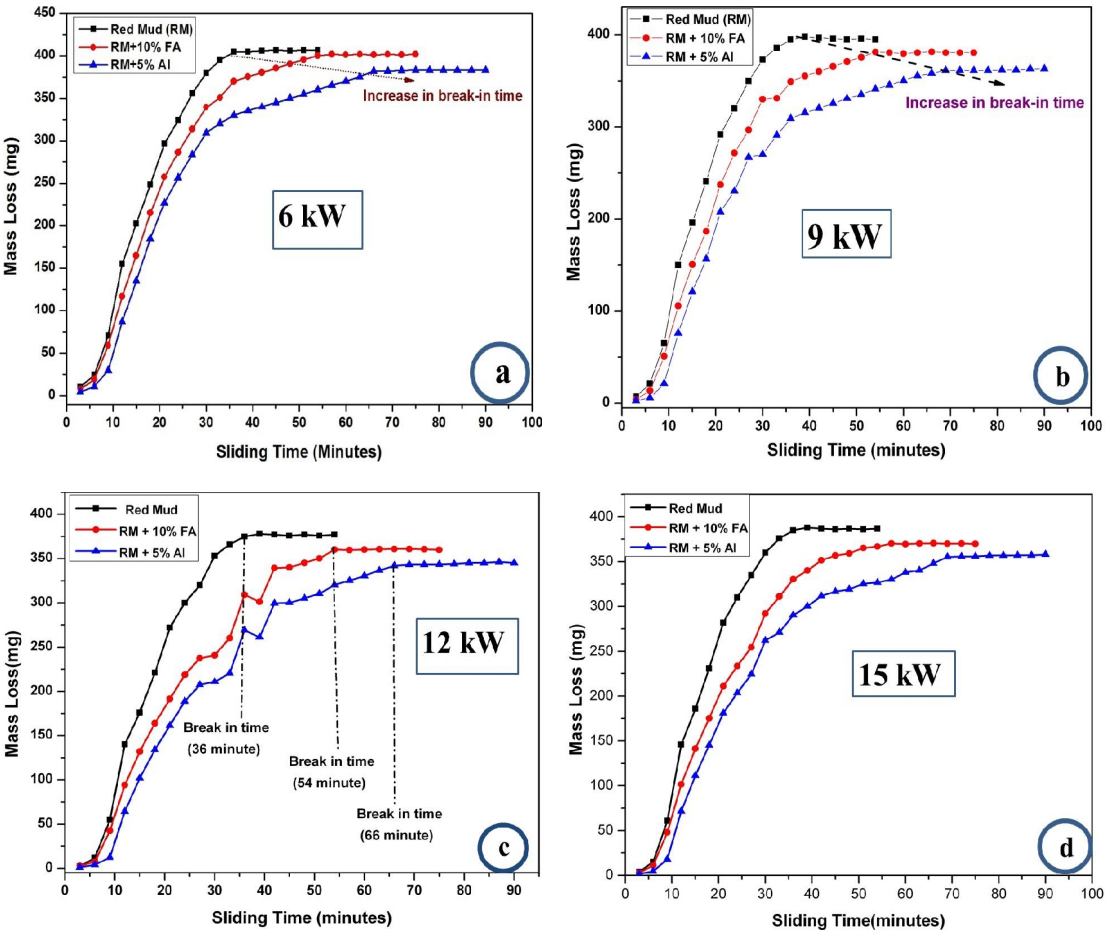

Fig. 15. Wear rate comparison for all coating type at different operating power level (a) 6 kW, (b) 9 kW , (c) 12 kW (d) 15 kW

The variation of wear rates (mass loss) for each coating type with sliding time were compared for different operating power level in (Fig. 15 above). This prominently displays a comprehensive recognition to the readers. From the results it is obvious that a significant growth in wear resistance was contrived with fly ash and aluminium addition to red mud resulting in stronger interfacial bond strength and dense film formation at boundary layer.

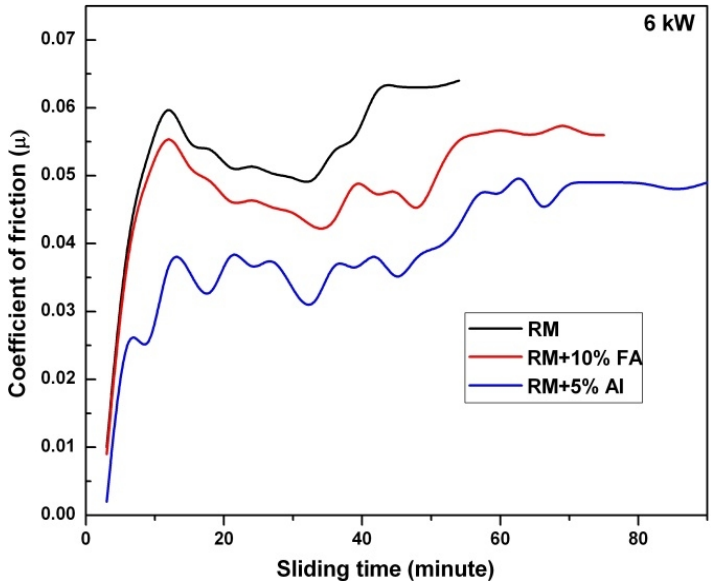

Fig. 16. Coefficient of friction for all Coating type at 6 kW

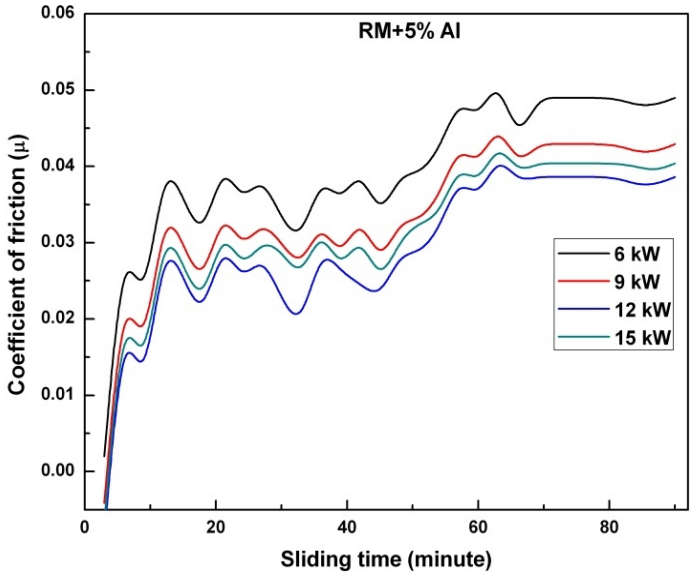

Fig. 17. Comparison of coefficient of friction for RM + 5% Al at all power level

A graphical representation concerning the variation of coefficient of friction with sliding time is also focused. At 6 kW operating power level and for all coating type the coefficient of

friction plot is presented in (Fig.16 above). For all sliding time the coefficient of friction is maximum for red mud and minimum for Red Mud + 5 % Al coating. At incipient, the frictional values are extreme followed by a curly trend and finally static values. Frictional values are compared for different operating power level for Red Mud + % 5 Al coating in (Fig. 17 above). As like mass loss an optimum operating power level also observed for friction coefficient. The effectiveness of frictional force is maximum at 6 kW and minimum at 12 kW was detected.

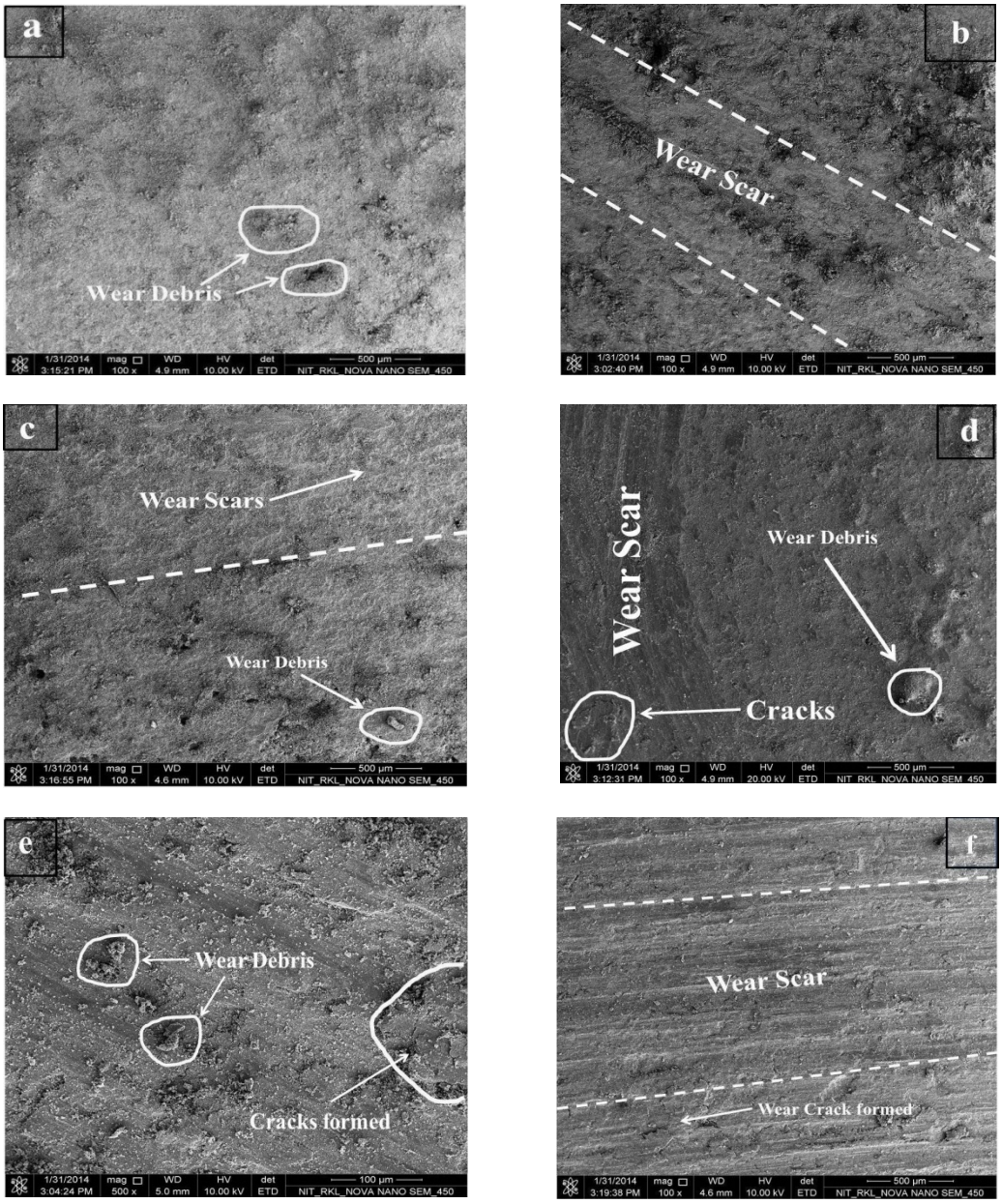

Fig. 18. Wear images for Red Mud + 5 % aluminium coating for 9 kW operating power level; considering (a) 15, (b) 30, (c) 45, (d) 60, (e) 75 and (f) 90 minutes time interval

Wear morphology for designated coating samples were emphasized using FESEM. (Fig. 18 above) illustrates the wear images for Red Mud + 5 % aluminium coating (for 9 kW operating power level) considering for time intervals of 15, 30, 45, 60, 75 and 90 minutes. Wear scars, debris and cracked sections formed are being visible. The wear morphology pattern modifies with time impacting the surface roughness leading to interruption of its contact mechanism. The wear characteristics recasts due to variation of hardness of the inter layers with time. After the break-in phase, increase in sliding distance cannot reform the contact area causing a relatively steady wear rate. Hence it can be winded up that the wear takes place by abrasion and adhesion mechanism due to development of shear stress in between hard particles of the two surfaces in contact. The same mechanism is relevant for all coating type.

4. CONCLUSION

The present experimental study remarks some noteworthy conclusions. Red mud, the waste generated from alumina plant is significantly coat able on mild steel using thermal plasma spraying technique with acceptable wear resistance. Addition of fly ash and aluminium with red mud diminishes the wear rate by amplifying the coating mechanism. It is observed that initially the wear rate increases at a slow pace and then boosted up with sliding distance for all coating type and finally becomes still. Operating power level authenticates as remarkable variable for coating property; which enriches the coating resistance, but eventually with reaching an optimum value indicating some other governing parameters. This work is a portfolio for future investigators to discover many other aspects of red mud and its composite coatings. Thermal security of these coatings may be evaluated for better claiming in high temperature applications. Corrosive wear behavior under different operating conditions may be explored to identify suitable application areas. Post heat treatment of these coatings may also be fetched to study regarding the improvement in coating features.

COMPETING INTERESTS

Authors have declared that no competing interests exist.

REFERENCES

1. Kushner BA, Novinski ER. Thermal spray coating. ASM Hand book. 1992;18(829-833).
2. Crook P. Friction and wear of hard facing alloy. ASM Hand book. 1992;18:(758-765).
3. Mishra SC, Das S, Satapathy Alok, Ananthapadmanabhan PV, Sreekumar KP. Erosion wear analysis of plasma sprayed ceramic coating using the taguchi technique. Tribology Transactions. 2009;52(3):401-404.
4. Mantry S, Jha BB, Satapathy A. Evaluation and characterization of plasma sprayed cu slag-al composite coatings on metal substrates. Journal of Coatings. 2013;7:842-865. DOI: 10.1155/2013/842865.
5. Afzal M, Ajmal M, Khan AN. Wear behavior of WC-12% co coatings produced by air plasma spraying at different standoff distances. Tribology Transactions. 2014;57(1):94-103.
6. Waynea SF, Sampath S, Anand V. Wear mechanisms in thermally sprayed mo-based coatings. Tribology Transactions. 1994;37(3):636-640.
7. Wang Y, Jin Y, Wen S. The analysis of the friction and wear mechanisms of plasma-sprayed coatings at 450°C. Wear. 1998;128:265–276.

8. Wang Y, Jin Y, Wen S. The analysis of the chemical structure and properties of ceramic surface films in friction using SEM, AES and Micro-region X-ray diffraction. Wear. 1998;128:277–290.
9. Wang Y, Jin Y, Wen S. The inspection of sliding surface and subsurface of plasma-sprayed using scanning acoustic microscopy. Wear. 1998;134:399–411.
10. Vijande-Diaz R, Belzunce J, Fernandez E, Rincon A, Pérez MC. Wear and microstructure in fine ceramic coatings. Wear. 1991;148:233–331.
11. Wei J, Xue Q. Effects of additives on friction and wear behaviour of Cr_2O_3 coatings. Wear. 1993;160:61–65.
12. Homberg K, Mathews A, Ronkainen H. Coatings tribology-contact mechanisms and surface design. Tribology International. 1998;31(1-3):107-120.
13. Sutar H, Mishra SC, Sahoo SK, Chakraverty AP, Maharana HS. Progress of red mud utilization: An overview. American Chemical Science Journal. 2014;4(3):255-279.
14. Sutar H, Mishra SC, Sahoo SK, Satapathy A, Kumar V. Morphology and solid particle erosion wear behaviour of red mud composite coatings. Natural Science. 2012;4(11):832-838.
15. Satapathy A, Sutar H, Mishra SC, Sahoo SK. Characterization of plasma sprayed pure red mud coatings: An analysis. American Chemical Science Journal. 2013;3(2):151-163.
16. Prasad N, Sutar H, Mishra SC, Sahoo SK, Acharya SK. Dry sliding wear behavior of aluminium matrix composite using red mud an industrial waste. International Research Journal of Pure and Applied Chemistry. 2013;3(1):59-74.
17. Satapathy A. Thermal spray coating of red mud on metals. PhD Thesis, National Institute of Technology, Rourkela, Odisha, India; 2005.
18. Bolton W. Higher engineering science. Routledge, New York. 2011;78.

Peer-review history:
The peer review history for this paper can be accessed here:
http://www.sciencedomain.org/review-history.php?iid=528&id=16&aid=5884